Applied Radiation and Isotopes 233 (2026) 112617

Contents lists available at ScienceDirect

Applied Radiation and Isotopes

journal homepage: www.elsevier.com/locate/apradiso

Assessment of indoor radon levels and annual effective dose across university campus: A case study from Kırşehir Province, Turkiye

Murat Dag

Vocational School of Health Services, Kirsehir Ahi Evran University, Kirsehir, 40100, Turkiye

ARTICLE INFO

Keywords:
Indoor radon level
Annual effective dose
CR-39
Kırşehir

ABSTRACT

This study presents a campus-wide assessment of indoor ^{222}Rn at Kırşehir Ahi Evran University (Central Anatolia, Türkiye), providing a measurement-based baseline for both the main campus and affiliated off-campus facilities. Indoor radon was monitored using CR-39 passive solid-state nuclear track detectors deployed across the main campus and the university's facilities in Kaman, Mucur, and Çiçekdağ, covering 46 measurement points within 17 buildings for at least three months. Radon activity concentrations ranged from 13 to 99 Bq/m^3 (overall mean: 32.46 Bq/m^3; median: 26.5 Bq/m^3); 58.7% of measurement points were below 30 Bq/m^3, and none exceeded 100 Bq/m^3. Substantial spatial heterogeneity was observed between buildings and across floor levels. Basements exhibited the highest mean concentration (~52.1 Bq/m^3), yet several buildings showed non-monotonic vertical profiles, indicating that ventilation practices and room-specific entry pathways may override simple height-dependent trends. Based on building-mean values, the annual effective dose ranged from 0.124 to 0.550 mSv/y (mean: 0.270 mSv/y), corresponding to an excess lifetime cancer risk (ELCR) of 0.434 - 1.925 × 10^{-3} (mean: 0.944 × 10^{-3}). Overall, these findings provide an institutional baseline to support follow-up monitoring and targeted ventilation optimisation.

1. Introduction

Environmental radioactivity arises from both natural and anthropogenic sources; however, natural background radiation remains the primary contributor to the cumulative dose received by the general population. The radionuclides of greatest radiological significance occur mainly in the long-lived uranium and thorium decay series in the Earth's crust. In the uranium series, ^{222}Rn is produced by the decay of ^{226}Ra (Fig. 1) and is especially important because, as a noble gas, it can emanate from mineral grains, migrate through porous media, and enter buildings via soil gas and ground-contact structural elements (Martin and McBride, 2012).

Radon is generated continuously from trace radium in rocks and soils and can reach the surface through several pathways, most notably diffusion and advective transport in soil gas, as well as groundwater transport followed by degassing to air. Because ^{222}Rn is chemically inert, colourless, odourless, and tasteless, it can accumulate without sensory warning; its relatively high atomic mass also means it is substantially denser than air, and it is therefore encountered at variable concentrations in soils, outdoor and indoor air, and natural waters (Kreuzer and McLaughlin, 2010).

For indoor exposure assessments, ^{222}Rn is the principal isotope of concern. Its half-life (≈3.8 days) is long enough to allow migration from source regions into occupied spaces, where concentrations may increase under limited ventilation. Accordingly, the present study focuses on ^{222}Rn and reports indoor activity concentrations together with estimates of annual effective dose and excess lifetime cancer risk (ELCR) under assumptions appropriate for ^{222}Rn-based assessment (Alpen, 1998).

From a public-health perspective, indoor ^{222}Rn is of particular concern because most of the dose arises not from the inert gas itself but from its short-lived progeny. After decay, these metallic daughters attach to airborne aerosols, are inhaled, and deposit in the respiratory tract, where subsequent alpha emissions deliver a highly localised dose to bronchial epithelium. This exposure pathway underpins the established association between long-term indoor radon exposure and lung-cancer risk (United Nations Scientific Committee on the Effects of Atomic Radiation, 2020). Consistent with this evidence base, the U.S. Environmental Protection Agency (EPA) (EPA, 2025) identifies radon as the leading cause of lung cancer among never-smokers and the second leading cause overall, while the World Health Organization (WHO) (WHO, 2023) estimates that radon contributes approximately 3% to 14% of lung cancers in a country depending on national average radon

E-mail address: muratdag@ahievran.edu.tr.

https://doi.org/10.1016/j.apradiso.2026.112617
Received 8 January 2026; Received in revised form 17 March 2026; Accepted 4 April 2026
Available online 9 April 2026
0969-8043/

levels and smoking prevalence.

Accordingly, systematic measurement of indoor ^{222}Rn concentrations provides an essential basis for exposure assessment and for prioritising ventilation optimisation and other mitigation actions in occupied buildings. Indoor ^{222}Rn concentrations exhibit pronounced spatial and temporal variability, driven by both geogenic source characteristics and building-specific determinants that control entry and dilution. At the source level, radon generation depends on local ^{226}Ra content and on the emanation of radon into pore space; subsequent transport is influenced by soil structure, permeability, and moisture conditions, as well as near-surface pressure and temperature gradients. Once radon reaches the building-ground interface, entry into indoor air occurs via diffusion and, frequently, pressure-driven flow through preferential pathways such as cracks in slabs, floor-wall junctions, construction joints, service penetrations, and drainage routes. Consequently, indoor concentration is typically governed primarily by the soil-to-indoor entry rate together with the ventilation (air-exchange) characteristics of the structure, rather than by construction materials alone. These mechanisms explain why elevated levels are often observed in basements and ground-contact rooms, while building envelope integrity, operational ventilation, heating practices, and occupancy behaviour can also produce substantial variability across floors and seasons (Institut de Radioprotection et de Surete Nucleaire - IRSN, 2018).

Therefore, to obtain representative mean concentrations and the associated annual effective dose under such variability, time-integrated measurements are generally the method of choice. Passive dosimetry using solid-state nuclear track detectors (SSNTDs), particularly CR-39, has therefore become a standard approach for indoor radon studies. CR-39 enables long-term integration without external power and is suitable for multi-location deployment; after exposure, chemical etching enlarges latent alpha tracks that can be counted optically and converted to ^{222}Rn activity concentration using an appropriate calibration factor. Concentration data can then be translated into annual effective dose by applying clearly defined assumptions for equilibrium factor and occupancy time that reflect the monitored micro-environments.

In parallel with the growing recognition of radon as a public-health concern, an extensive body of literature has reported indoor ^{222}Rn measurements and associated dose estimates across diverse building types and climatic-geological settings. Comparable assessments have been conducted both across different regions of Türkiye (Büyükuslu et al., 2018; ÇAKMAK et al., 2023; Can et al., 2012; Celik et al., 2008; Haner et al., 2010; Karakiliç et al., 2009; Sogukpinar et al., 2014) and worldwide (Abd-elzaher, 2012; Ahmad et al., 2018; Al-Naggar et al., 2024; Angelova et al., 2023; Hashim et al., 2021; Hashim and Mohammed, 2016; Janik et al., 2023; Kandari et al., 2016; Luca et al., 2022; Mazur et al., 1999; Mohammad and Al-Zubaidy, 2012; Pantelić et al., 2019; Quarto et al., 2015; Sowby, 1981; Younis et al., 2020), motivated by the need to characterise population exposure, identify high-radon micro-environments, and inform mitigation strategies. However, campus-focused datasets remain limited for many provinces and site-specific building stocks. This limitation is important because university campuses comprise heterogeneous buildings and functional spaces. University campuses represent a distinctive indoor setting for radon assessment because they comprise heterogeneous building stocks and diverse functional spaces-administrative offices, classrooms, laboratories, libraries, and communal areas-with different ventilation regimes and occupancy schedules. Students and staff may spend extended periods indoors, making campus buildings relevant for routine exposure assessment and institutional indoor air-quality management. Importantly, within-campus variation can be substantial; therefore, building-specific measurements are often more informative than reliance on regional averages alone.

Region-specific baseline data are particularly valuable for Central Anatolia, where local geology, construction practices, and ventilation behaviours may yield indoor exposure patterns that differ from those reported elsewhere. In this context, the present study reports the first campus-wide survey of indoor ^{222}Rn at Kırşehir Ahi Evran University, conducted using CR-39 passive solid-state nuclear track detectors (SSNTDs). Indoor ^{222}Rn activity concentrations and the associated annual effective dose are quantified across the main campus and affiliated campuses in Kırşehir Province, Türkiye, thereby establishing a reference baseline for future monitoring and mitigation. The specific objectives are to: (i) characterise the distribution of indoor ^{222}Rn concentrations across representative campus buildings and occupied microenvironments; (ii) estimate annual effective dose under clearly defined, university-relevant occupancy scenarios; and (iii) identify spatial patterns and potential high-radon locations that may warrant ventilation optimisation, targeted mitigation, or follow-up surveillance. The outcomes are intended to support evidence-based campus indoor air-quality management and to contribute robust baseline data to the regional radon literature in Türkiye.

2. Method

Indoor ^{222}Rn activity concentration was measured using Radosys passive radon dosimeters equipped with a CR-39 solid-state nuclear track detectors (SSNTDs) supplied by NUKEN, TENMAK (Ankara). The dosimeter is a compact, screw-cap diffusion-chamber device (26 × 55 mm) designed for indoor measurements. It is based on an air-gap filter diffusion-chamber concept, and the diffusion chamber is made of conductive plastics to provide electrostatic protection. The CR-39 detector chip has an active area of 1 cm^2 and is mounted beneath the cap, as seen in Fig. 2 (Radosys Kft, 2012).

Field measurements were conducted in buildings on the Main Campus of Kırşehir Ahi Evran University and at the university's off-campus facilities in Kaman, Mucur, and Çiçekdağ, covering 17 locations and 46 measurement points. Geographic coordinates were

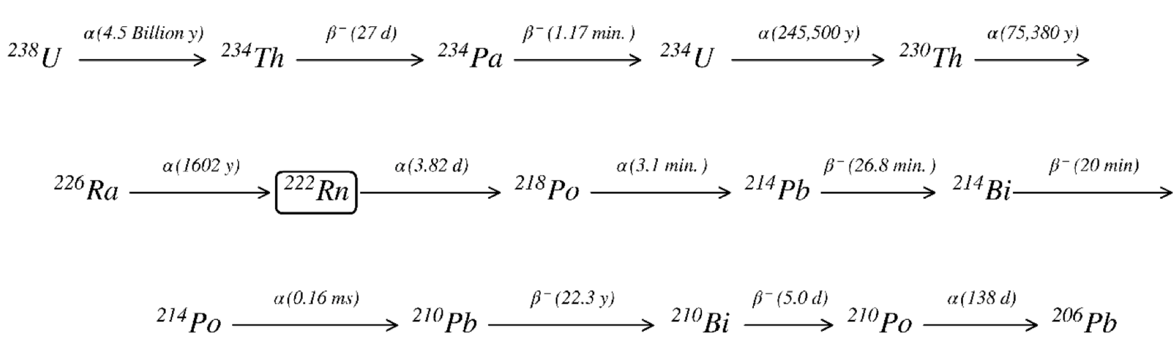

Fig. 1. Schematic representation of the ^{238}U decay series from ^{238}U to stable ^{206}Pb. Nuclides are shown as circles annotated with their half-lives, while arrows indicate the decay mode (α or β). The key indoor-exposure radionuclide ^{222}Rn is highlighted.

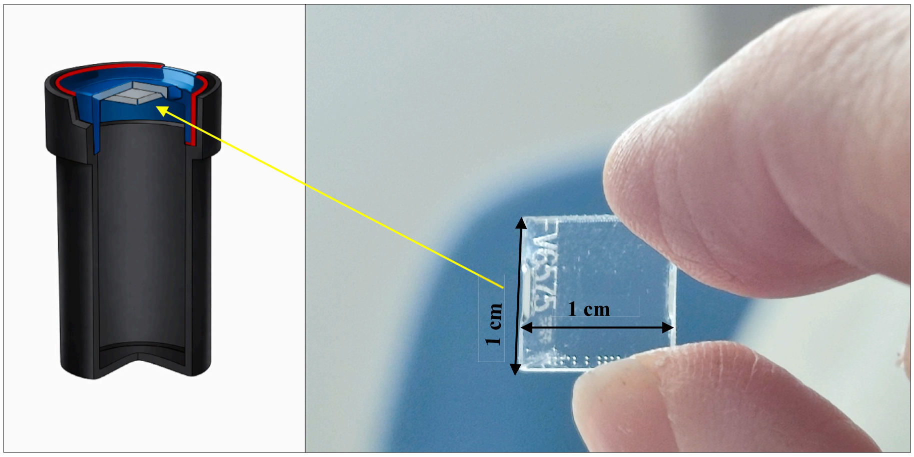

Fig. 2. 3D model of the Radosys radon dosimeter equipped with a CR-39 nuclear track detector. The schematic cross-section (left) shows the detector placement beneath the screw cap, while the photograph (right) presents the 1 cm × 1 cm x 1 mm (thickness) CR-39 detector chip used for alpha-track registration.

$$C_{Rn} = \frac{CF \cdot D_{Rn}}{T} \cdot \frac{1000}{24} \quad \text{Eq. 1}$$

recorded in DMS format for each location, and measurements were stratified by floor level (basement, ground, first, and second floors) to capture the expected influence of ground coupling and vertical transport.

Dosimeters were installed at approximately 1.7 m above floor level, away from doors and windows, in the rooms of selected buildings, and were deployed on 21–22 July 2025 and retrieved on 6–7 November 2025, corresponding to an exposure duration of 107–108 days. All monitored rooms were normally occupied offices/administrative rooms without mechanical ventilation systems; air exchange occurred via doors and/or windows under normal daily use (opening frequency not monitored). After exposure, each diffusion chamber was resealed in its original airtight aluminium pouch at the same measurement location. The individually sealed pouches were then placed in a dedicated box additionally covered/shielded with aluminium foil and transported to the NUKEN, TENMAK (Ankara) radon laboratory for processing and analysis.

Laboratory processing and optical readout were performed using a Radosys radon measurement system (Radosys Ltd, 2013), a Radobath unit for chemical etching, and a Radometer 2000 computer-aided evaluation unit. As part of the analysis preparation procedure, CR-39 detectors were chemically etched in a 6.25 M NaOH solution at 90 ± 3 °C for 4.5 h. Following etching, the detectors were removed from the solution, thoroughly rinsed with pure water, and allowed to dry. The detectors were then analysed using the Radometer 2000 evaluation unit. Track-density determination was performed via automated scanning with the Radometer software: each CR-39 detector was processed on a 1/144 stepwise grid, and alpha tracks were automatically identified and counted under a microscope-based magnified imaging system(Fig. 3). To assess measurement repeatability, each detector was read five times under identical scanning conditions. As is well known, alpha-particle incidence at different angles can produce tracks ranging from near-circular to elliptical morphologies. In this work, track identification and counting were performed using the Radometer 2000 system and the vendor-provided algorithm installed with the system at the NUKEN, TENMAK radon laboratory, under fixed, identical scanning conditions. Calculations of the radon activity concentration in the sample, expressed in becquerels per cubic metre (C_{Rn}), were performed using the following relationship.where CF denotes the calibration factor, T is the exposure duration in days, and D_{Rn} is the measured track density attributed to radon. Using this procedure, the ambient radon concentration in air is determined in units of Bq/m^3, consistent with the

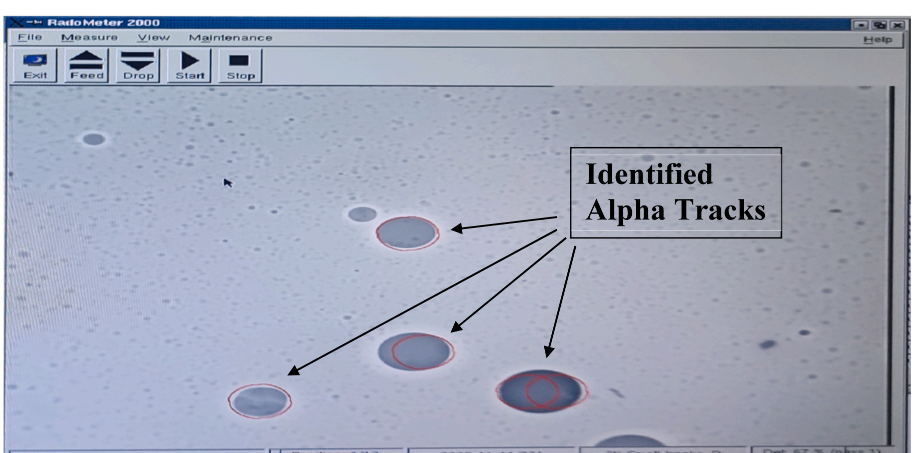

Fig. 3. Representative Radometer 2000 (Radosys) analysis screen illustrating the automated identification of alpha-particle tracks on an etched CR-39 detector; detected tracks are highlighted (circled) by the software for subsequent track-density determination.

underlying radioactive-decay principles. Here, m^3 represents the reference unit volume of the enclosed environment, while the becquerel (Bq) is the SI unit of activity, corresponding to one nuclear decay per second. The measured track densities were subsequently converted into radon activity concentrations using the formula as seen in Eq. (1), and presented in Table 1. According to the manufacturer's specification, detectors are supplied fully assembled in an airtight pouch with Al-vapor finish and each unit is sealed individually into an airtight/radon-proof pouch in N_2 atmosphere; the typical initial background is reported as 0.3 tracks·mm^{-2} ("Radosys - RSKS detector," 2013). A separate blank/control-detector determination of intrinsic background track density (processed and scanned in parallel) was not performed in this study.

3. Results

3.1. Indoor radon activity concentrations and summary statistics

During the monitoring, CR-39 passive dosimeters were deployed at 17 locations (46 measurement points) across Kırşehir Ahi Evran University campuses and remained in place over three months (from 21 to 22 July to 6-7 November 2025). The Radon Activity Concentrations (RAC, Bq/m^3), together with the associated standard deviations (SD) and relative uncertainties (Unc., %), are reported by location, coordinates (DMS), and floor level in Table 1. The measured RAC values range from 13 to 99 Bq/m^3, with an overall mean of 32.46 Bq/m^3 and a median of 26.5 Bq/m^3. Most measurement points fall within the low-to-moderate range: 27 out of 46 (58.7%) are $<$30 Bq/m^3, 13 out of 46 (28.3%) lie in the 30-49 Bq/m^3 interval, and 6 out of 46 (13.0%) are $\geq$50 Bq/m^3. Notably, two basement-level points reached 99 Bq/m^3, representing the upper end of the dataset but still below commonly applied reference levels for indoor radon.

3.2. Spatial patterns (campus/building) and floor-level dependence

Clear spatial variability is observed among campuses and buildings (Table 1), as seen Figs. 4 and 5. The highest campus-level averages occur at Mucur VSH (44-71 Bq/m^3; mean ~56.7 Bq/m^3) and Çiçekdağ VSH (25-69 Bq/m^3; mean ~44.3 Bq/m^3). In the Main Campus subset (34 points), the distribution is broader (13-99 Bq/m^3; mean ~30.7 Bq/m^3) and highlights distinct hotspots. The Faculty of Sport Sciences shows consistently elevated values across floors (99, 53, 44 Bq/m^3), and the

Table 1
Indoor radon activity concentration (RAC, Bq/m^3) measured with CR-39 dosimeters at the indicated locations and floor levels, together with the corresponding standard deviation (SD) and relative uncertainty (Unc., %) for measurement points across Kırşehir Ahi Evran University campuses (Mucur, Çiçekdağ, and Kaman) and selected buildings on the Main Campus; geographic coordinates are reported in DMS format.

NO	LOCATION	COORDINATES	FLOOR	RAC (Bq/m^3)	SD	UNC. (%)
1	Mucur Vocational School	39° 03′ 42.48″ N 34° 23′ 14.39″ E	Basement	44	6.877	5.66%
2			Ground	71	5.683	2.89%
3			First	55	2.408	1.59%
4	Çiçekdağ Vocational School	39° 36′ 36.29″ N 34° 24′ 43.28″ E	Ground	25	2.408	3.54%
5			First	69	1.304	0.68%
6			Second	39	3.435	3.23%
7	School Of Foreign	39° 08′ 39.50″ N 34° 07′ 30.88″ E	Basement	31	1.924	2.29%
8			Ground	26	5.762	7.89%
9			First	16	2.168	4.90%
10	Neşet Ertaş Faculty of Fine Arts	39° 08′ 21.24″ N 34° 07′ 04.73″ E	Ground	39	3.391	3.17%
11			First	36	0.894	0.90%
12	Faculty of Medicine	39° 08′ 15.83″ N 34° 07′ 09.44″ E	Basement	28	7.232	9.34%
13			Ground	23	4.722	7.31%
14			First	26	5.167	7.26%
15			Second	30	2.55	3.07%
16	Physiotherapy Vocational School	39° 08′ 19.53″ N 34° 07′ 21.27″ E	Ground	33	1.924	2.13%
17			First	13	2.28	6.55%
18			Second	19	8.289	15.94%
19	Faculty of Engineering & Architecture	39° 08′ 33.30″ N 34° 07′ 11.29″ E	Basement	99	2.387	0.87%
20			Ground	23	1.581	2.47%
21			First	17	6.708	13.98%
22	Faculty of Arts & Sciences	39° 08′ 34.48″ N 34° 07′ 22.00″ E	Ground	21	5.541	9.42%
23			First	27	4.324	5.77%
24	Faculty of Education	39° 08′ 29.33″ N 34° 07′ 19.29″ E	Ground	17	5.177	10.92%
25			First	13	4.393	12.41%
26			Second	14	3.05	7.74%
27	Faculty of Agriculture	39° 08′ 36.20″ N 34° 07′ 15.91″ E	Basement	20	7.259	12.92%
28			Ground	29	4.848	6.14%
29	Faculty of Sport Sciences	39° 08′ 41.01″ N 34° 07′ 21.92″ E	Basement	99	6.261	2.30%
30			Ground	53	3.162	2.18%
31			First	44	7.162	5.89%
32	Central Research Lab.	39° 08′ 38.13″ N 34° 07′ 26.02″ E	Basement	44	2.302	1.91%
33			Ground	45	7.335	5.90%
34	Central Library	39° 08′ 32.57″ N 34° 07′ 30.44″ E	Ground	37	3.536	3.50%
35			First	16	3.347	7.40%
36			Second	21	3.05	5.22%
37	Faculty of Theology	39° 08′ 24.29″ N 34° 07′ 29.60″ E	Ground	20	2.683	4.99%
38			First	28	3.271	4.20%
39			Second	15	3.162	7.91%
40	IT Center	39° 08′ 24.21″ N 34° 07′ 20.96″ E	Ground	20	4.97	8.84%
41	Kaman Vocational School	39° 21′ 26.23″ N 33° 42′ 3.96″ E	Ground	17	1.581	3.44%
42			First	22	3.493	5.75%
43			Second	36	7.765	7.88%
44	Kaman Applied Sciences Vocational School	39° 21′ 22.16″ N 33° 41′ 50.14″ E	Ground	18	6.76	13.31%
45			First	24	3.536	5.44%
46			Second	31	11.649	13.51%

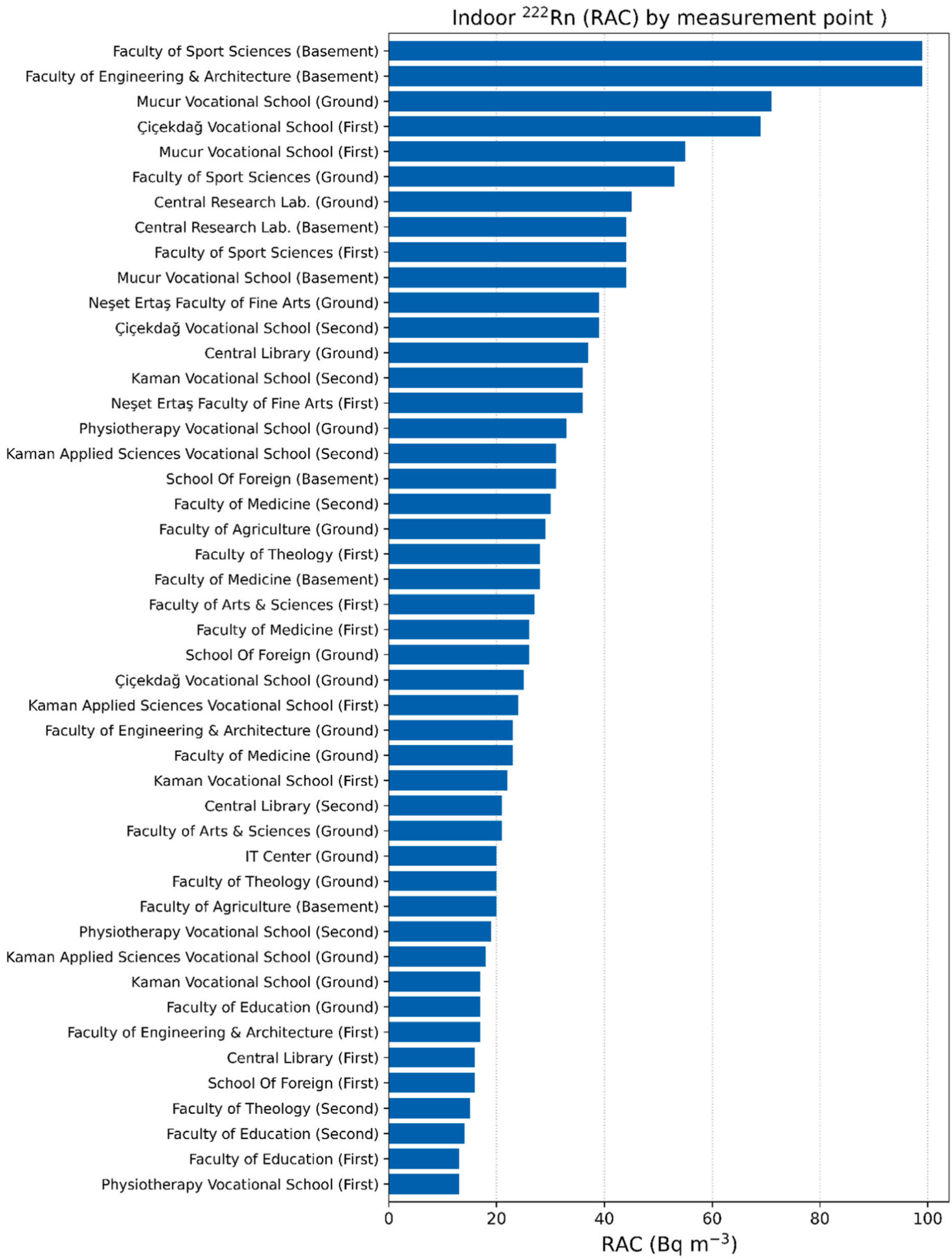

Fig. 4. Indoor ^{222}Rn activity concentration (RAC, Bq/m^3) at the 46 measurement points (labelled by location and floor; ranked).

Faculty of Engineering & Architecture includes one basement value at 99 Bq/m^3 but also much lower upper-floor readings (down to 17 Bq/m^3), underscoring pronounced within-building heterogeneity likely linked to room-specific ventilation, occupancy patterns, and ground-coupled entry routes.

When grouped by floor level, the expected tendency for higher radon at ground-coupled levels is evident in the aggregated statistics derived from Table 1, as seen in Fig. 6. Basement measurements (n = 7) yield the highest mean (~52.1 Bq/m^3), compared with ground (n = 17; ~30.4 Bq/m^3), first (n = 14; ~29.0 Bq/m^3), and second floors (n = 8; ~25.6 Bq/m^3). This pattern is consistent with established radon ingress mechanisms, where entry through cracks, floor–wall junctions, and service penetrations often produces higher concentrations in basements and other spaces in contact with the ground. However, several locations

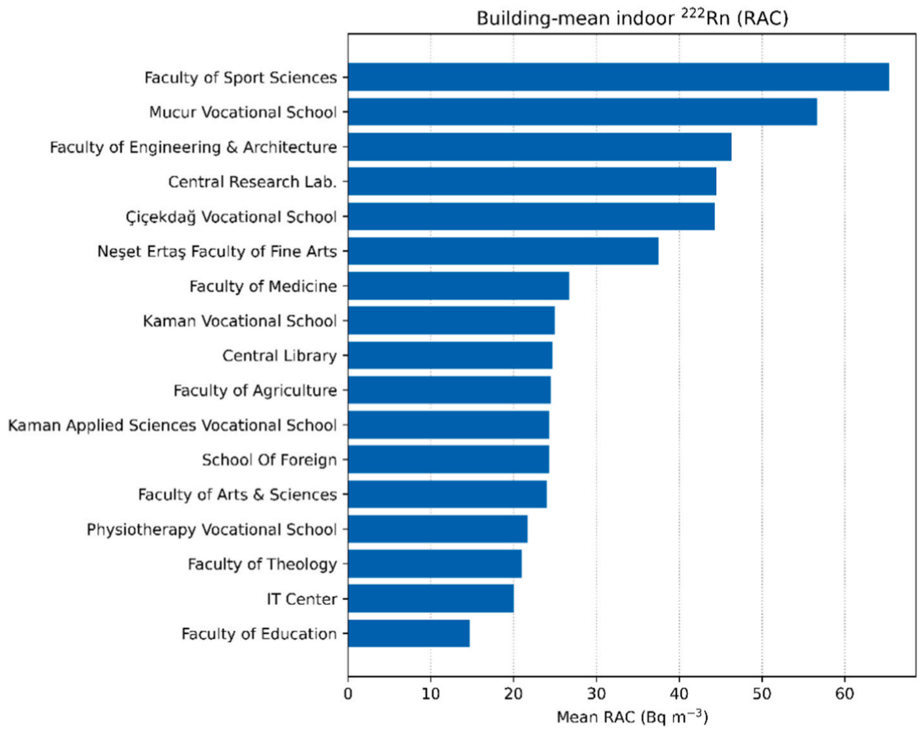

Fig. 5. Building-mean indoor ^{222}Rn activity concentration (RAC, Bq/m^3) for the 17 monitored buildings (ranked).

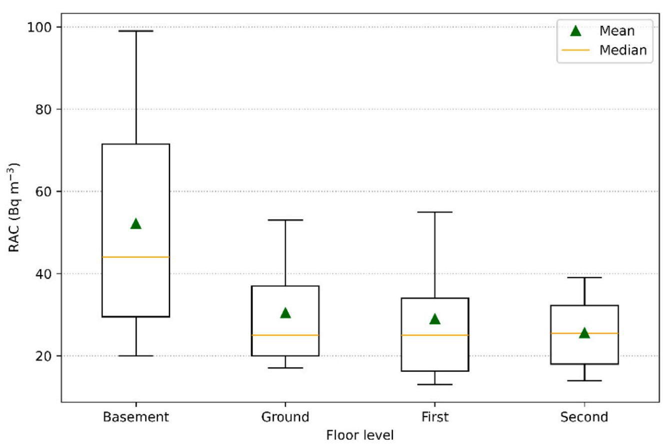

Fig. 6. Indoor ^{222}Rn activity concentration (RAC, Bq/m^3) by floor level shown as boxplots. The orange line denotes the median and the green triangle denotes the mean. (For interpretation of the references to colour in this figure legend, the reader is referred to the Web version of this article.)

do not follow a strictly monotonic vertical gradient (e.g., Mucur VSH and Çiçekdağ VSH show peaks on upper floors), which is plausible given that indoor radon can vary substantially between rooms and floors depending on ventilation regime, building layout, pressure differentials, and usage characteristics. The monitored university buildings are predominantly reinforced-concrete and brick structures, constructed in different periods. Differences in building age, tightness, and the presence of cracks/penetrations at floor–wall junctions may contribute to floor-to-floor variability by modulating radon entry pathways; however, this study did not include a systematic material-specific characterization (e.g., exhalation measurements), so material effects are discussed qualitatively. Across buildings completed between 2006 and 2023 (Table 2), construction year did not show a clear monotonic association with building-mean RAC (Spearman's $\rho = -0.245$, $p = 0.342$), and likewise no clear linear association was observed (Pearson's $r = -0.273$, $p = 0.289$). This supports the interpretation that, within the present scope, ground coupling together with room-specific ventilation/pressure conditions and building-specific entry pathways may dominate over construction year as a single predictor. This supports the interpretation that, within the present scope, ground coupling together with room-specific ventilation/pressure conditions and building-specific entry pathways may dominate over construction year as a single predictor.

Table 2
Mean indoor radon activity concentration (RAC, Bq/m^3) and the corresponding annual effective dose (AED, mSv/y) and excess lifetime cancer risk (ELCR) for the monitored buildings at Kırşehir Ahi Evran University. The building completion year is given in parentheses after each location name. AED values were calculated using Eq. (2). ELCR values were derived using Eq. (3) and are reported as $\times 10^{-3}$ for clarity.

No	Location	RAC (Bq/m^3)	AED (mSv/y)	ELCR x 10^{-3}
1	Mucur Vocational School (2016)	56.67	0.477	1.670
2	Çiçekdağ Vocational School (2015)	44.33	0.373	1.305
3	School Of Foreign (2015)	24.33	0.205	0.717
4	Neşet Ertaş Faculty of Fine Arts (2018)	37.50	0.316	1.106
5	Faculty of Medicine (2017)	26.75	0.225	0.788
6	Physiotherapy Vocational School (2016)	21.67	0.183	0.640
7	Faculty of Engineering and Architecture (2017)	46.33	0.390	1.365
8	Faculty of Arts and Sciences (2019)	24.00	0.202	0.677
9	Faculty of Education (2017)	14.67	0.124	0.434
10	Faculty of Agriculture (2017)	24.50	0.206	0.721
11	Faculty of Sport Sciences (2009)	65.33	0.550	1.925
12	Central Research Lab. (2010)	44.50	0.375	1.312
13	Central Library (2023)	24.67	0.208	0.728
14	Faculty of Theology (2021)	21.00	0.177	0.619
15	IT Center (2012)	20.00	0.168	0.588
16	Kaman Vocational School (2010)	25.00	0.211	0.738
17	Kaman Applied Sciences Vocational School (2006)	24.33	0.205	0.717

The repeatability metrics further support these interpretations. Each detector was read five times under identical scanning conditions, and the SD and Unc.(%) values reported in Table 1 provide a practical indication of measurement variability at each point. Across the dataset, SD ranges from 0.894 to 11.649 Bq/m^3 (mean ~4.32 Bq/m^3), while relative uncertainty spans 0.68% to 15.94% (mean ~6.10%). Higher relative uncertainties are generally associated with lower RAC values (where counting statistics and spatial heterogeneity have a proportionally larger effect), whereas the highest RAC results include some of the lowest uncertainties (e.g., 99 Bq/m^3 with Unc. 0.87-2.30%), indicating that the elevated concentrations at those hotspot basements are reproducible in repeated scans.

3.3. Annual effective dose and excess lifetime cancer risk under workplace occupancy time assumptions

To place the measured RAC values into the annual effective dose (AED) attributable to indoor ^{222}Rn exposure was estimated using a standard dose-conversion relationship (Eq. (2)) (Nations Scientific Committee on the Effects of Atomic RadiationU., 2000),

$$AED = C_{Rn} \,.\, F \,.\, O \,.\, DCF \quad \text{Eq. 2}$$

where C_{Rn} is the indoor radon activity concentration (Bq/m^3), F is the equilibrium factor between ^{222}Rn and its short-lived progeny (taken as 0.4), O is the indoor occupancy time (h/y), and DCF is the dose conversion factor (9 nSv/h per (Bq/m^3), i.e., 9.0x10^{-6} mSv/h per (Bq/m^3)). Because this investigation is campus-based rather than residential, occupancy was defined to reflect a typical full-time university presence (9 h/day x 5 days/week x 52 weeks/y), yielding O = 2340 h/y. Under these assumptions, Eq. (2) simplifies to AED (mSv/y) = 0.008424 x C_{Rn} (Bq/m^3). Using the overall mean concentration (C_{Rn} = 32.46 Bq/m), the corresponding AED is 0.273 mSv/y, while the median concentration (26.5 Bq/m^3) gives 0.223 mSv/y. Across the full observed range of the corresponding AED can be seen in Table 2).

For comparability with occupational radon–progeny metrics, exposure was additionally expressed in Working Level (WL) and Working Level Month (WLM). Using the equilibrium-equivalent concentration, defined as the progeny-equivalent concentration under an assumed equilibrium factor ($C_{EEC} = C_{Rn} \times F$), the progeny concentration was estimated as $WL = (C_{Rn} \times F)/3700$, where 3700 Bq/m^3 is the conventional equilibrium-equivalent concentration corresponding to 1 WL. The annual exposure rate was then calculated as WLM/y = WL × (O /170), where 170 h represents the standard "working month" used in the definition of WLM. With F = 0.4 and O = 2340 h/y, this simplifies to WLM/y = 0.001488 × C_{Rn}, corresponding to approximately 0.019–0.147 WLM/y across the measured concentration range (mean ≈ 0.048 WLM/y).

Excess lifetime cancer risk (ELCR) was additionally calculated as a screening-level indicator derived from cumulative effective dose over a nominal lifetime (Eq. (3)),

$$ELCR = AED \,.\, DL \,.\, RF \quad \text{Eq. 3}$$

where DL is the duration of life (70 y) and RF is the nominal risk factor (0.05 Sv^{-1}). Converting AED from mSv to Sv (10^{-3}) yields ELCR = AED (mSv/y) x 0.00335, and ELCR values are reported in Table 2 as x10^{-3} for clarity.

4. Conclusion

This study provides an on- and off-campus, measurement-based baseline of indoor ^{222}Rn across Kırşehir Ahi Evran University using CR-39 passive SSNTDs deployed at 46 measurement points within 17 buildings/locations for an exposure period of at least three months. Point measurements of radon activity concentration (RAC) ranged from 13 to 99 Bq/m^3, with an overall mean of 32.46 Bq/m^3 and a median of 26.5 Bq/m^3. The distribution was dominated by low-to-moderate values (58.7% < 30 Bq/m^3; 28.3% in 30–49 Bq/m^3; 13.0% ≥ 50 Bq/m^3), and no point exceeded 100 Bq/m^3; therefore, the dataset remains within the WHO-recommended reference level of 100 Bq/m^3 (and well below 300 Bq/m^3). The measurements were obtained between 21 and 22 July 2025 and 6–7 November 2025 (≈107–109 days), providing a time-integrated estimate of indoor ^{222}Rn under typical university workplace conditions. Monitoring was confined to normally occupied office/administrative rooms without mechanical ventilation; air exchange occurred via doors and/or windows under routine use, and the frequency of opening/closing was not tracked.

Although overall concentrations were modest, the results demonstrate pronounced spatial heterogeneity between locations and within individual buildings. The expected influence of ground coupling is reflected in higher basement concentrations on average, yet non-monotonic floor-to-floor behaviour in some buildings indicates that room-specific ventilation, pressure differentials, and operational conditions can dominate a simple vertical-gradient expectation. Confidence in these patterns is reinforced by the readout protocol (five repeated scans per detector under identical conditions), which yielded pointwise SD and relative uncertainty metrics and did not suggest that hotspot values were artefacts of unstable counting. Interpretation of floor-to-floor behaviour should therefore be anchored in both ground coupling and building-specific operational and structural factors. The building stock is predominantly reinforced-concrete and brick and was completed in different periods; accordingly, differences in building age and tightness, together with potential entry pathways at floor–wall junctions and service penetrations, may contribute to the observed non-monotonic profiles alongside ventilation- and pressure-driven effects. Material-specific quantitative assessment (e.g., exhalation measurements) was not undertaken and remains a logical component of targeted follow-up at comparatively elevated locations.

Annual effective dose and risk indicators were evaluated using an explicit campus-appropriate occupancy scenario rather than a residential assumption. With F = 0.4, DCF = 9 nSv/h per (Bq/m^3), and O = 2340 h/y, the mean concentration corresponds to AED ≈ 0.270 mSv/y (median: 0.208 mSv/y), with an AED range of 0.124 - 0.550 mSv/y. Using DL = 70 years and RF = 0.05 Sv^{-1}, the corresponding ELCR are 0.944x10^{-3} (mean) and 0.728x10^{-3} (median), ranging roughly 0.434 – 1.925x10^{-3}. These dose and risk values should be interpreted strictly within the stated time–activity pattern, noting that AED and ELCR scale linearly with occupancy.

Accordingly, the study fulfils the objectives set out in the Introduction by (i) characterising the distribution of indoor ^{222}Rn across representative campus buildings and occupied microenvironments, (ii) quantifying annual effective dose under explicitly defined, university-relevant workplace occupancy assumptions, and (iii) resolving spatial patterns that highlight a small number of comparatively elevated locations where ventilation optimisation and/or targeted mitigation may be prioritised. By providing a campus-wide, measurement-based reference dataset, these findings establish a baseline against which future surveys can be benchmarked, support evidence-based indoor air-quality management at the university scale, and contribute robust institutional data to the regional ^{222}Rn literature in Türkiye.

Declaration of competing interest

The authors declare the following financial interests/personal relationships which may be considered as potential competing interests: Murat Dag reports financial support was provided by Kirsehir Ahi Evran University Scientific Research Projects. Reports a relationship with that includes:. Has patent pending to. If there are other authors, they declare that they have no known competing financial interests or personal relationships that could have appeared to influence the work reported in this paper.

Acknowledgements

This study was supported by Kırşehir Ahi Evran University Scientific Research Projects (BAP) under Project No. SAG.A2.25.002, Turkiye

Data availability

The data that has been used is confidential.

References

Abd-elzaher, M., 2012. An overview on studying ^{222} Rn exhalation rates. Am. J. Appl. Sci. 9, 1653–1659.

Ahmad, S., Ajaz, M., Ali, Y., Younis, H., Khan, K.H., Tabassum, U., 2018. Measurement of indoor radon concentration in district mardan, Khyber Pakhtunkhwa, Pakistan. Nucl. Phys. At. Energy 19, 190–195. https://doi.org/10.15407/jnpae2018.02.190.

Çakmak, N., Kanbur, U., Aal-Shabeeb, K.H.M., Erer, A.M., 2023. Radon concentration and its indices in bulak (Mencilis) cave. Bitlis Eren Univ. J. Sci. Technol. 13, 76–92. https://doi.org/10.17678/beuscitech.1248490.

Al-Naggar, T.I., Mohamed, S.E., Khan, A., Abdalla, A.M., 2024. Radiological assessment of radon and radium concentrations in Najran region soils, Saudi Arabia. J. Radiat. Res. Appl. Sci. 17, 100906. https://doi.org/10.1016/j.jrras.2024.100906.

Alpen, E.L., 1998. Radiation biophysics (second edition) chapter 16 - radiation exposure from natural background and other sources. Radiat. Biophys. 424–460.

Angelova, A., Chobanova, N., Kunovska, B., Djunakova, D., Ivanova, K., Stojanovska, Z., 2023. Radon exposure in kindergartens in one Bulgarian district. Nukleonika 68, 51–56. https://doi.org/10.2478/nuka-2023-0007.

Büyükuslu, H., Özdemir, F.B., Öge, T.Ö., Gökce, H., 2018. Indoor and tap water radon (^{222}Rn) concentration measurements at Giresun University campus areas. Appl. Radiat. Isot. 139, 285–291. https://doi.org/10.1016/j.apradiso.2018.05.027.

Can, B., Albayrak, N., Canbazoğlu, C., Çelebi, N., Doğru, M., 2012. Measurements of indoor radon concentration levels in Kilis, Osmaniye and antakya, Turkey during spring season. J. Radioanal. Nucl. Chem. 292, 1059–1063. https://doi.org/10.1007/s10967-011-1559-z.

Celik, N., Cevik, U., Celik, A., Kucukomeroglu, B., 2008. Determination of indoor radon and soil radioactivity levels in Giresun, Turkey. J. Environ. Radioact. 99, 1349–1354. https://doi.org/10.1016/j.jenvrad.2008.04.010.

Epa, U., 2025. Health risk of radon | US EPA [WWW Document]. URL. https://www.epa.gov/radon/health-risk-radon, 1.6.26.

Haner, B., Yilmaz, A., Kürkçüoğlu, M.E., Karadem, A., Üniversitesi, Z.K., Yüksekokulu, Z. M., Karaelmas Üniversitesi, Z., Fakültesi, F.E., Bölümü, F., Üniversitesi, S.D., Alınış, T., 2010. Mencilis (Bulak) Mağarasında Radon Seviyesi Ölçümleri.

Hashim, A.K., Najam, L.A., Aljomaily, F.M.A., 2021. Contribution of soil in the annual effective dose due to radon in the air of some dwellings in the city of Karbala, Iraq. Pol. J. Med. Phys. Eng. 27, 233–239. https://doi.org/10.2478/pjmpe-2021-0028.

Hashim, A.K., Mohammed, E.J., 2016. Measurement of radon concentration and the effective dose rate in the soil of the city of Karbala. Iraq. J. Radiat. Nucl. Appl. 1, 17–23. https://doi.org/10.18576/jrna/010103.

Institut de Radioprotection et de Surete Nucleaire - IRSN, P.S. et E. 31 avenue de la D.L. 92260 F.-R. (France), 2018. New Dose Coefficients for Radon Recommended by the CIPR in its Publication 137. Explanatory note.

Janik, M., Bossew, P., Hasan, M.M., Cinelli, G., 2023. Indoor Radon research in the Asia-Pacific Region. Atmosphere 14, 1–24. https://doi.org/10.3390/atmos14060948.

Kandari, T., Aswal, S., Prasad, M., Bourai, A.A., Ramola, R.C., 2016. Estimation of annual effective dose from radon concentration along main boundary Thrust (MBT) in Garhwal himalaya. J. Radiat. Res. Appl. Sci. 9, 228–233. https://doi.org/10.1016/J.JRRAS.2015.10.005.

Karakiliç, V., Bayraktar, G., Kürkçüoğlu, E., Haner, B., Yilmaz, A., Merkezi'nde, S.D.Ü.B., Ölçümleri, R., 2009. Radon measurements at S.D.U. information center. Journal of Natural and Applied Sciences.

Kreuzer, M., McLaughlin, J., 2010. Radon - WHO guidelines for indoor air quality: selected pollutants - NCBI bookshelf [WWW Document]. URL. https://www.ncbi.nlm.nih.gov/books/NBK138712/, 1.6.26.

Luca, A., Rădulescu, I., Ioan, M.R., Fugaru, V., Teodorescu, C., Barna, C., Tuţă, C.S., Tugulan, C.L., Antohe, A., Lalău, I., Cîmpeanu, C., Postolache, C., 2022. Recent progress in radon metrology at IFIN-HH, Romania. Atmosphere 13. https://doi.org/10.3390/atmos13030363.

Martin, P., McBride, J.L., 2012. Radionuclide behaviour and transport in the tropical atmospheric environment. Radioact. Environ. Times 18, 59–91. https://doi.org/10.1016/B978-0-08-045016-2.00002-3.

Mazur, D., Janik, M., Łoskiewicz, J., Olko, P., Swakoń, J., 1999. Measurements of radon concentration in soil gas by CR-39 detectors. Radiat. Meas. 31, 295–300. https://doi.org/10.1016/S1350-4487(99)00135-3.

Mohammad, A.I., Al-Zubaidy, N.N., 2012. Estimation of natural radioactivity in water and soil in some villages of Irbid city. Appl. Phys. Res. 4, 39–47. https://doi.org/10.5539/apr.v4n3p39.

Nations Scientific Committee on the Effects of Atomic Radiation, U., 2000. Sources And Effects Of Ionizing Radiation Annex B Exposures from Natural Radiation Sources.

Pantelić, G., Čeliković, I., Živanović, M., Vukanac, I., Nikolić, J.K., Cinelli, G., Gruber, V., 2019. Qualitative overview of indoor radon surveys in Europe. J. Environ. Radioact. 204, 163–174. https://doi.org/10.1016/j.jenvrad.2019.04.010.

Quarto, M., Pugliese, M., Verde, G. La, Loffredo, F., Roca, V., Quarto, M., Pugliese, M., Verde, G. La, Loffredo, F., Roca, V., 2015. Radon exposure assessment and relative effective dose estimation to inhabitants of puglia region, south Italy. Int. J. Environ. Res. Publ. Health 12, 14948–14957. https://doi.org/10.3390/IJERPH121114948, 2015, Vol. 12, Pages 14948-14957.

Radosys Kft, 2012. RADOSYS user manual [WWW Document]. URL. http://www.radosys.com/index_htm_files/RSKS_RS_Man82-130129_c.pdf, 1.8.26.

Radosys Ltd, 2013. Radosys - Radon [WWW Document]. URL. http://www.radosys.com/radon-page1.htm, 1.6.26.

Sogukpinar, H., Algin, E., Asici, C., Altinsoz, M., Cetinkaya, H., 2014. Seasonal indoor radon concentration in Eskisehir, Turkey. Radiat. Protect. Dosim. 162, 410–415. https://doi.org/10.1093/rpd/nct344.

Sowby, F.D., 1981. Annals of the ICRP. Ann. ICRP 6, 1. https://doi.org/10.1016/0146-6453(81)90127-5.

United Nations Scientific Committee on the Effects of Atomic Radiation, 2020. UNSCEAR 2000 report scientific annex B: lung cancer from exposure to radon. UNSCEAR 2019 Report, Sci. Annex B, Lung cancer from Expo. to radon I, 1–282.

WHO, 2023. Radon [WWW Document]. URL. https://www.who.int/news-room/fact-sheets/detail/radon-and-health, 1.5.26.

Younis, H., Qureshi, A.A., Wazir, Z., Mehboob, K., Ajaz, M., 2020. Measurement of indoor radon concentration in the hunza valley of karakoram ranges northern Pakistan. Iran. J. Sci. Technol. Trans. A Sci. 44, 1153–1159. https://doi.org/10.1007/s40995-020-00904-5.